

Supplemental Information: Symmetry Enforced Fermi Surface Degeneracies Observed in TRSB Superconductor LaNiGa_2 with ARPES

Matthew Staab, Robert Prater, Sudheer Sreedhar, Journey Byland, Eliana Mann, Davis Zackaria, Yunshu Shi, Henry Bowman, Yundi Quan, Warren Pickett, Valentin Taufour, and Inna Vishik

(Dated: October 16, 2023)

In this work, some presented spectra are reconstructed by stacking many spectra together at varying deflector angles. This is in contrast to typical spectra whose angle (parallel momentum) axis is along a detector slit. The reconstructed spectra are the following: Figure 4 (b) panels, Figure 5 (b) panels, Figure 6 (b) panels.

CRYSTAL ALIGNMENT

Laue diffraction utilizes reflections of a polychromatic X-ray beam to orient single crystals. X-rays whose wavelength satisfy the Laue equations (Bragg condition) with the lattice are coherently reflected and form bright spots on the detector. These diffraction spots can then be used to easily orient the crystal, especially if one knows the crystal symmetry beforehand. In Figure 1, we show the Laue image for LaNiGa_2 . The a and c axes are identified by the four smallest-angle reflected peaks separated by 90 degrees. After alignment, samples are scored along that axis in order to preserve alignment when performing ARPES and mounting samples for the thin edge cleave. Inset in Figure 1 is an image of the sample that is aligned with respect to the Laue image shown.

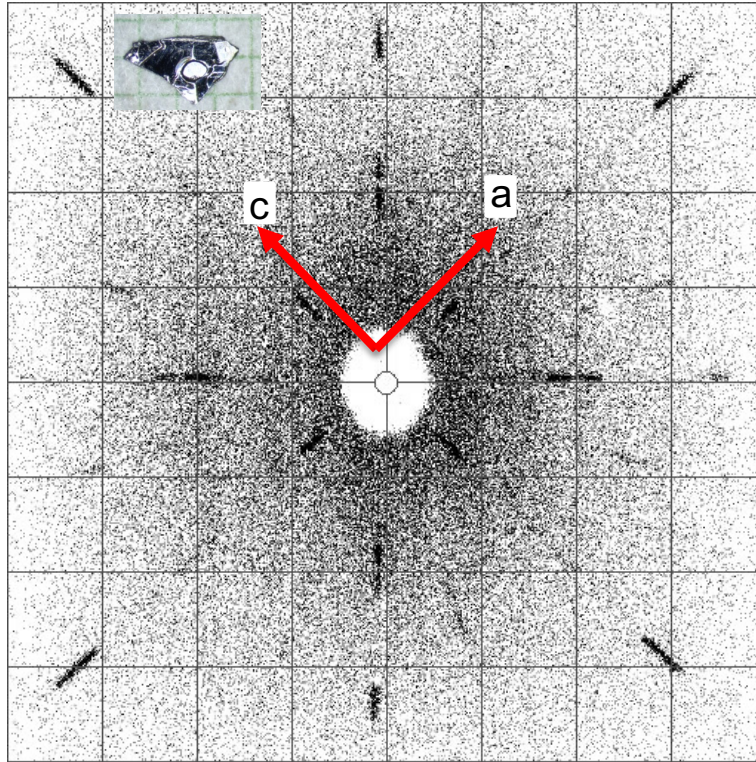


FIG. 1. Laue image of LaNiGa_2 sample showing the orientations of the \vec{a} and \vec{c} axes. This orientation allows for samples to be mounted on the thin edge with the desired axis normal to the sample holder. Inset shows the sample on mm paper that is rationally aligned with the Laue image.

DETERMINING k_{\perp}

ARPES uses conservation of energy as well as momentum to probe electronic structure of materials. In the case of momenta parallel to the surface, there is no change in potential along that direction so momentum conservation is trivial, modulo a momentum kick from the photon which is only relevant at much higher photon energy than presently employed. However, in the case of momentum perpendicular to the surface, there is a potential discontinuity due to the termination of the crystal. That additional change provides an extra term to the relevant energy for determining the momentum. As given in equation 1 below the additional term V_0 , called the inner potential, is generally found by finding the periodicity as a function of photon energy [1].

$$k_{\perp} = \frac{1}{\hbar} \sqrt{2m(E_{kin} \cos^2 \theta + V_0)} \quad (1)$$

Here, we determine the value of the inner potential to be $15eV$ in order to align features seen in the photon energy dependence of spectra with the following justifications:

(1) Photon energy dependent stacked Fermi crossings, as seen in SI Figure 4 provide a rough guide to the inner potential. However, because the observed bands are quasi-2D they do not constrain the inner potential more than $V_0 \approx 17 \pm 3eV$. Further attempts were made with other locations in the BZ with similar results.

(2) Dispersion tracking as a function of photon energy, as seen in SI Figure 2. A band is reconstructed along k_{perp} and compared to band structure calculations. V_0 is adjusted to yield the best agreement between experiment and theory.

Strategies (1) and (2) allowed us to constrain the inner potential to be $V_0 \approx 15 \pm 1eV$. Any further constraint would require multiple BZs of periodicity to ascertain.

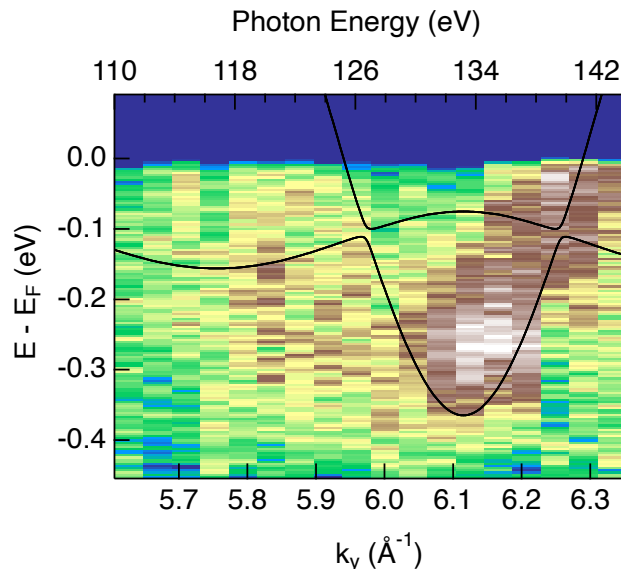


FIG. 2. **Photon energy dispersing band.** EDCs taken along the k_z zone boundary ($k_x = 0$) were stacked at many photon energies which reconstructs the $Z - T$ line from measurements on a natural cleave. The perpendicular momentum (k_y) is displayed along the bottom axis using an inner potential of $15eV$.

Figure 4 was created by taking photon energy dependent spectra from $110eV$ to $144eV$. These spectra show evolving fermiology and matrix elements as a function of photon energy. Near the Gamma plane at $114eV$ we see FS3 extremely bright while FS2 has strongly diminished matrix element. However, at a photon energy of $120eV$, features attributed to FS2 become clearly distinguishable again. With these spectra, the momentum dependent intensity was integrated near the Fermi level and then projected onto k_y vs k_x using equation 1. The Fermi surface maps at each of the photon energies is shown in Figure 3. The nodal plane is oriented at constant k_z for each panel, same as similar Figures in the main text, and 'X' shaped features are clearly seen on the nodal plane in most of the Fermi surface maps, as further evidence of the distinct fermiology of this space group.

In the main text, we showed bands merging as individual cuts approach the nodal plane, and in Fig. 4 we demonstrate the same for an entire plane. This Figure shows constant energy contours as a function of perpendicular momentum near and on the k_z BZ boundary along with their respective DFT overlays. This Figure was reconstructed from data collected in the natural cleave geometry. In this image, the most prominently observed bands are those corresponding to calculated bands FS4/5. There is a clear merging of bands at the BZ boundary as predicted by the DFT calculations across the whole probed plane.

To ascertain which perpendicular momentum is probed with $144eV$ in the thin-edge cleave (k_x in this orientation), we compared the obtained Fermi surface maps with the DFT calculations at multiple values of k_x . Three nearby values of k_x are shown in Figure 5. Just a 0.08\AA^{-1} difference in k_x changes makes a dramatic difference in the Fermiology, and at $k_x = 0.08\text{\AA}^{-1}$, there are experimental features, particularly along $k_y = 0\text{\AA}^{-1}$ which are no longer captured by the calculations, as compared to the good fit for $k_x = 0\text{\AA}^{-1}$ and $k_x = 0.04\text{\AA}^{-1}$. Because a constant kinetic energy probes a sphere in momentum space, the true difference in measured k_x from the center of the zone to the k_z boundary ($\approx 0.7\text{\AA}^{-1}$) is approximately 0.05\AA^{-1} . That curvature along with the agreement of observed Fermiology to the DFT calculations on the $k_x = 0\text{\AA}^{-1}$ plane allow us to determine that a photon energy of $144eV$ probes the $k_x = 0\text{\AA}^{-1}$ plane within an uncertainty of $\approx 0.04\text{\AA}^{-1}$.

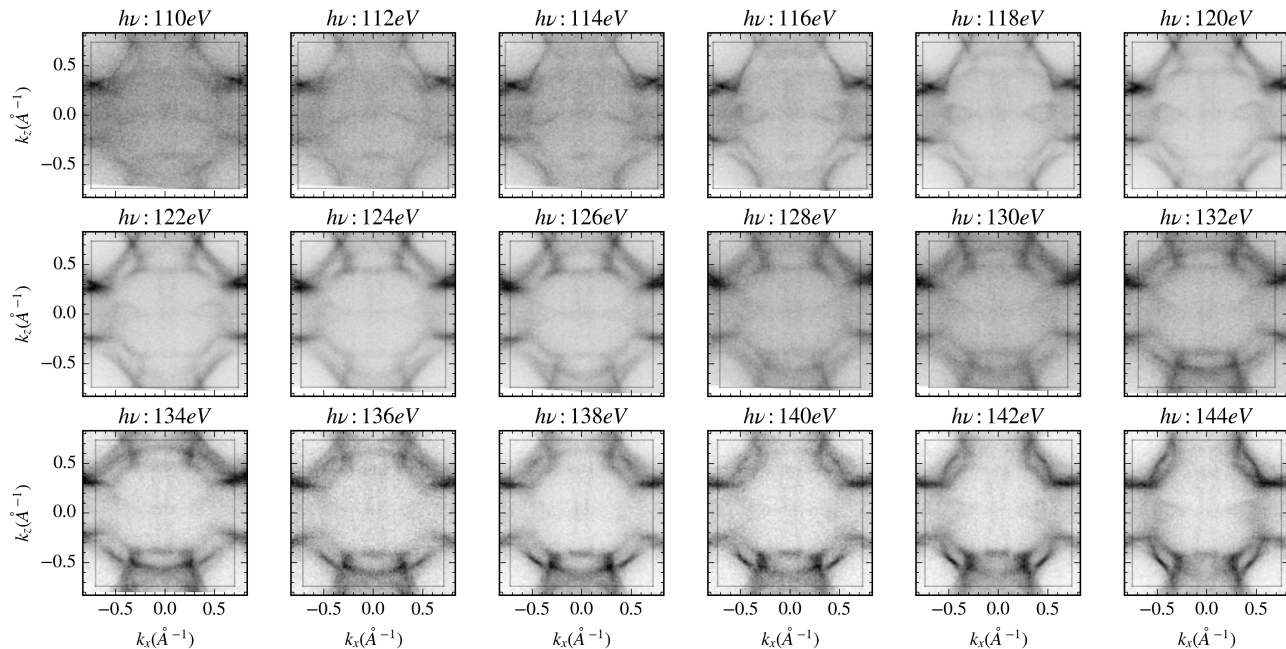


FIG. 3. **Constant energy maps at multiple photon energies** Fermi surface maps integrated $50meV$ around the Fermi energy are shown at a range of photon energies from $110eV$ to $144eV$ in steps of $2eV$. Gray box in each Figure outlines the Brillouin zone boundary at that photon energy as determined by an inner potential of $15eV$.

In Figure 7 we show a broad XPS scan of $LaNiGa_2$ taken at a photon energy of $144eV$. This spectrum shows all of the expected peaks for La , Ni , and Ga with the addition of possible contamination of Al from the growth as well as Au which was evaporated on the sample prior to cleaving in order to provide a Fermi level reference.

REFERENCES

- [1] A. Damascelli, Physica Scripta **2004**, 61 (2004).

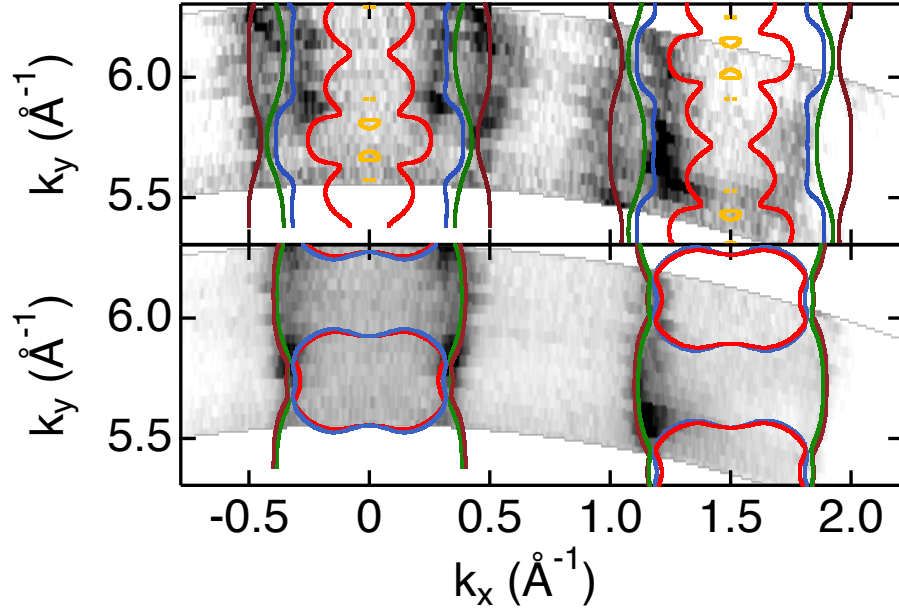


FIG. 4. **Photon energy dependence of and near the $Z - T - A$ plane.** Similar to Figure ??, the top and bottom panel show constant binding energy contour ARPES maps over a range of photon energies from 110eV to 144eV . (Top) k_x near the BZB boundary, at the location shown by the solid red line in main text Figure ?? (c). (Bottom) On the $k_z = \pi/c$ plane, probing the SOC split Dirac lines and loop. Overlaid on both are the DFT calculated Fermi crossings.

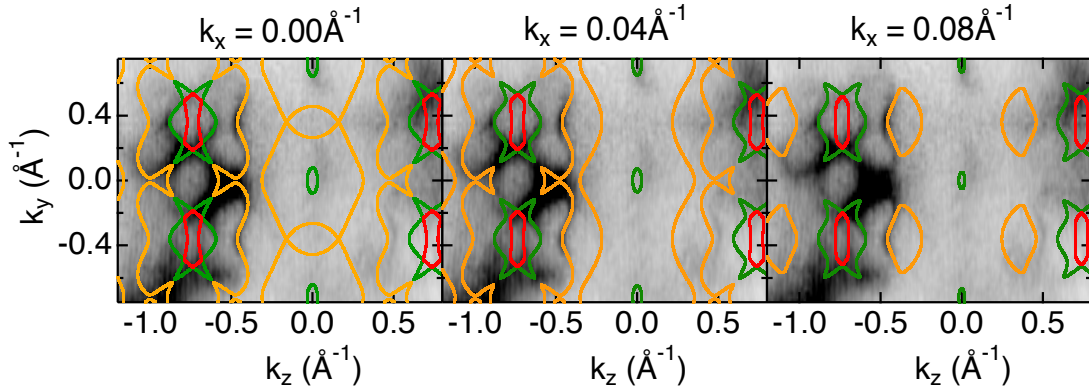


FIG. 5. **Comparison of Thin-edge 144eV Fermi Surface with Nearby Theory** The black and white ARPES data is the same for all panels. It is a constant energy contour at the Fermi energy taken on the thin edge with a photon energy of 144eV . The three panels are overlaid with DFT calculations from different k_x values, showing that the data agrees most with $k_x = 0$.

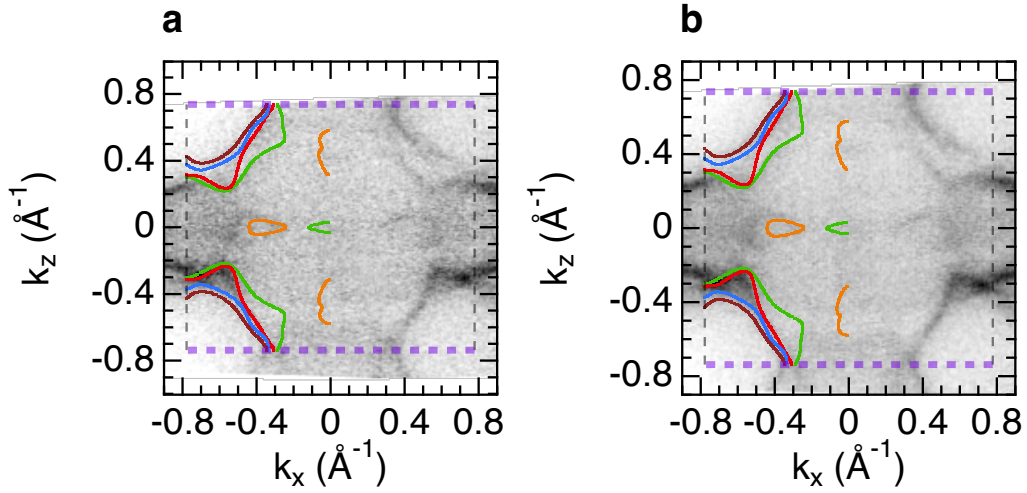


FIG. 6. **Comparison of Energy Integration Windows** (a) Fermi surface map using a photon energy of 116eV and integrated 15meV around the Fermi level. (b) Same as (a) with an integration window of 50meV . Both panels have overlaid the calculated Fermi surface on the left half of the data. Black and purple dashed lines indicate the BZ boundary along the k_x and k_z directions respectively.

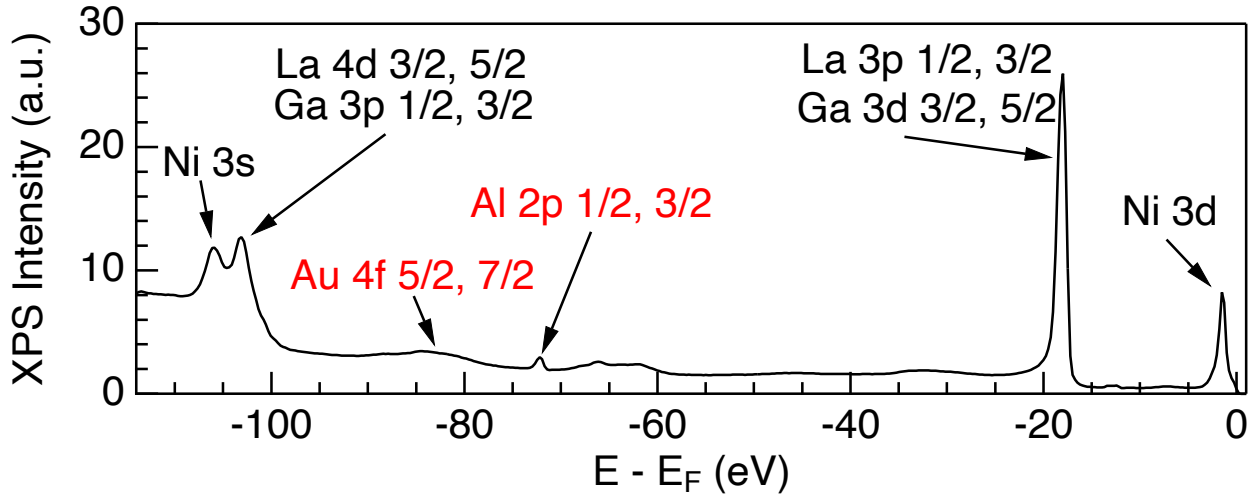


FIG. 7. **XPS of LaNiGa_2** The XPS spectrum was taken at 144eV . Black annotations show the locations of all known La , Ni , and Ga peaks in the shown binding energy range. The red annotations show the locations of likely contaminant atoms from the growth and sample preparation methods to explain unexpected peaks.